JGR Atmospheres

RESEARCH ARTICLE
10.1029/2019JD030575

Special Section:
Bridging Weather and Climate: Subseasonal-to-Seasonal (S2S) Prediction

Impact of the QBO on Prediction and Predictability of the MJO Convection

Shuguang Wang[1], Michael K. Tippett[1], Adam H. Sobel[1,2], Zane K. Martin[1], and Frederic Vitart[3]

[1]Department of Applied Physics and Applied Mathematics, Columbia University, New York, NY, USA, [2]Lamont-Doherty Earth Observatory, Columbia University, Palisades, NY, USA, [3]European Centre for Medium-Range Weather Forecasts, Reading, UK

Key Points:
- Prediction skill of boreal winter MJO convection is higher by 5–10 days in QBO easterly than QBO westerly in the WMO/S2S models
- Model forecasted stratosphere has little influence on MJO prediction
- BSISO prediction skill in QBO westerly is higher than easterly in 2000–2010 but reverses before 1999

Supporting Information:
- Supporting Information S1

Correspondence to:
S. Wang,
sw2526@columbia.edu

Citation:
Wang, S., Tippett, M. K., Sobel, A. H., Martin, Z., & Vitart, F. (2019). Impact of the QBO on prediction and predictability of the MJO convection. *Journal of Geophysical Research: Atmospheres*, *124*, 11,766–11,782. https://doi.org/10.1029/2019JD030575

Received 4 MAR 2019
Accepted 21 SEP 2019
Published online 21 NOV 2019

Author Contributions:
Conceptualization: Shuguang Wang
Data curation: Shuguang Wang
Formal analysis: Shuguang Wang
Funding acquisition: Shuguang Wang
Investigation: Shuguang Wang
Methodology: Shuguang Wang, Michael K. Tippett, Adam H. Sobel
Project administration: Shuguang Wang
Resources: Shuguang Wang
Software: Shuguang Wang
Supervision: Shuguang Wang
Validation: Shuguang Wang
Visualization: Shuguang Wang
Writing - original draft: Shuguang Wang, Michael K. Tippett, Adam H. Sobel, Zane K. Martin, Frederic Vitart
(continued)

Abstract The impact of the quasi-biennial oscillation (QBO) on the prediction of tropical intraseasonal convection, including the Madden Julian Oscillation (MJO) and Boreal Summer Intraseasonal Oscillation (BSISO), is assessed in the WMO Subseasonal to Seasonal (S2S) forecast database using the real-time OLR based MJO (ROMI) index. It is shown that the ROMI prediction skill for the boreal winter MJO, measured by the maximum time at which the anomaly correlation coefficient exceeds 0.6, is higher by 5 to 10 days in the QBO easterly phase than its westerly phase. This difference occurs even in models with low tops and poorly resolved stratospheres. MJO predictability, as measured by signal to noise ratio in the S2S ensemble, also shows a similar difference between the two QBO phases, and results from a simple linear regression model show consistent behavior as well. Analysis of the ROMI index derived from observations indicates that the MJO is more coherent and stronger in the QBO easterly phase than in the westerly phase. These results suggest that the skill dependence on QBO phase results from the initial state of the MJO, the regularity of its propagation in the verifying observations, or most likely a combination of the two, but not on an actual stratospheric influence on the MJO within the model simulations. In contrast to the robust QBO-MJO connection in boreal winter, the BSISO prediction skill exhibited by the S2S models in boreal summer is greater in the QBO *westerly* phase than in the *easterly* phase during the 1999 to 2010 period. This is consistent with the observation that BSISO OLR anomalies are stronger in the QBO westerly phase during that period. However, this relationship between the QBO and BSISO in boreal summer changes in recent decades: BSISO is weaker in QBO westerly than easterly during 1979–2000. Correspondingly, the QBO impact on BSISO prediction in boreal summer also reverses in that period as well in a statistical model, whereas this statistical model shows a consistent QBO impact on MJO prediction in boreal winter over the past four decades.

1. Introduction

The Madden-Julian Oscillation (MJO; Madden & Julian 1971, 1972; Xie et al., 1963; Li et al., 2018) is the dominant mode of intraseasonal variability in the tropics. It influences weather directly over large regions of the tropics and subtropics, and its influence extends to the midlatitude and polar regions via Rossby wave trains excited by MJO convection. Understanding of the MJO's predictability is of great value.

One factor which has recently emerged as important to the MJO is the quasi-biennial oscillation (QBO; Baldwin et al., 2001) in the tropical stratosphere. A number of recent studies have found strong statistical relationships between the QBO phase and the amplitude of the MJO in northern winter. Yoo and Son (2016) and Son et al. (2017) showed that the MJO variance is higher in the QBO easterly phase (EQBO) than in the QBO westerly phase (WQBO) in boreal winter. Zhang and Zhang (2018) argued that the QBO has its strongest impact when the MJO convection anomaly is centered over the Maritime Continent.

These recent findings on the MJO-QBO connection have important consequences for MJO prediction. Marshall et al. (2017) showed that the QBO-MJO connection modulates MJO prediction skill in a subseasonal numerical weather prediction (NWP) model with prediction skill of the Real-Time Multivariate MJO index (RMM; Wheeler & Hendon, 2004) being higher in the QBO easterly phase and lower in the QBO westerly phase. Marshall et al. (2017) also examined the QBO influence as a function of the initial amplitude of the MJO in the forecasts. They found that the difference in MJO prediction skill between QBO phases remains when forecasts with the same initial MJO amplitudes are compared, suggesting that the skill difference is not a simple consequence of higher-amplitude MJO initial conditions in the easterly phase.

Writing – review & editing: Shuguang Wang, Michael K. Tippett, Adam H. Sobel, Zane K. Martin, Frederic Vitart

While studies to date are broadly consistent in finding a QBO influence on MJO prediction and predictability, understanding of this influence is limited. The QBO may influence both initial and boundary conditions, and their relative roles in influencing the MJO are not clear. For example, there is abundant evidence that air-sea turbulent fluxes at the lower boundary play important roles in the prediction of the MJO (DeMott et al., 2015). It is plausible that the QBO wind/temperature signature in the upper troposphere/lower stratosphere (UT/LS) region may reduce errors near the tropopause—which we may think of as an "upper boundary" for the tropospheric MJO—thereby improving prediction. On the other hand, given that there is a statistical relationship between QBO phase and MJO amplitude in observations, the QBO influence may be implicit in the tropospheric initial conditions, and influence the MJO prediction through that pathway. This influence could then be independent of the extent to which the QBO influences the MJO during the model run, or the QBO is even present in a given NWP model at all—especially considering that some NWP models have poorly resolved stratospheres. It is desirable to understand whether this is the case, both to inform prediction and model development strategies (e.g., whether a well-resolved stratosphere is important to MJO prediction) and because it may help to understand the physical mechanism by which the QBO influences the MJO, which also remains unclear at present.

Another aspect of the MJO-QBO connection is the seasonal dependence of the QBO-MJO relationship. Yoo and Son (2016) found that the QBO-MJO relationship is significant in boreal winter but not in boreal summer. It is possible that this seasonal contrast is due to the distinctly different characteristics of the MJO in these two seasons. The intraseasonal oscillation mostly propagates eastward in northern winter, when its convection anomalies are focused south of, but close to, the equator. In northern summer, when its convection anomalies are primarily found north of the equator, it propagates both northward and eastward, and reaches latitudes further from the equator than in northern winter. Because of these different characteristics, the MJO in summer is also referred to as the Boreal Summer Intraseasonal Oscillation (BSISO) in the literature. Densmore et al. (2019) further examined the QBO-MJO relationship in different seasons, and found—in addition to the documented signal in northern winter—that the QBO can also impact the MJO in other seasons in certain MJO phases, that is, when the MJO convection is over the Maritime Continent in boreal spring and summer. It is of interest to see how this complex seasonality may influence the predictability of intraseasonal convective anomalies associated with the MJO in boreal winter and BSISO differently across the seasonal cycle.

The purpose of this study is to explore the QBO influence on the prediction and predictability of tropical intraseasonal convection anomalies using observations and the World Meteorological Organization's (WMO) S2S retrospective forecast data set (Vitart et al., 2017). We use the real-time OLR based MJO index (OMI, or ROMI for the real-time variant; Kiladis et al., 2014) in order to focus on convection—as opposed to the circulation anomalies which are emphasized by some other indices, including RMM—and we examine predictability across the seasonal cycle, including how it changes over the duration of the record. Lim et al. (2019) recently showed robust QBO influence on the RMM index prediction skill during the boreal winter in the S2S data set. Our study is complementary to that study, and expands upon the relationship between intraseasonal convection variability and the seasonal cycle.

The rest of this article is structured as follows: section 2 contains a brief description of the S2S models used here, the indices for diagnosing the MJO and QBO, and a linear regression model for the MJO. Section 3 discusses the QBO impact on prediction and predictability of intreaseasonal convection anomalies. Section 4 summarizes this paper.

2. Method and the S2S Data

2.1. The S2S Prediction Database

Reforecasts of the MJO were obtained from the WMO's Subseasonal-to-seasonal (S2S) Prediction Project database (Vitart 2017). Most of the reforecasts are integrated for more than 30 days for subseasonal prediction. Table 1 summarizes the forecast configurations of the 10 S2S models used in this study: the Australian Bureau of Meteorology (BoM), the China Meteorological Administration (CMA), the European Centre for Medium-Range Weather Forecasts (ECMWF), Environment and Climate Change Canada (ECCC), the Institute of Atmospheric Sciences and Climate of the National Research Council (CNR-ISAC), the Hydrometeorological Centre of Russia (HMCR), the Japan Meteorological Agency (JMA), Météo-France/

Table 1
S2S Model Configurations: Horizontal and Vertical Resolutions of the Model Atmospheres, Model Tops, Reforecast Types, Forecast Periods, Reforecast Frequencies, and Ensemble Sizes

	Resolution	Model top	Rfc type	Rfc period	Rfc frequency	Ens size	O/A coupling
BOM	~T47 L17	10 hPa	F	1981–2013	Sixper month	3 × 11	Y
CMA	T106 L40	0.5 hPa	F	1994–2013	Daily	4	Y
CNR-ISAC	0.75 × 0.56 L54	~6.8 hPa	F	1981–2010	Every five days	1	slab
CNRM	T255L91	0.01 hPa	F	1993–2013	Two per month	15	Y
ECCC	0.45 × 0.45 L40	2 hPa	O	1995–2013	Weekly	4	persistent SST
ECMWF	T639/319 L91	0.01 hPa	O	1996–2013 (past 20 years)	Two per week	11	Y
HMCR	1.1 × 1.4 L28	5 hPa	O	1985–2010	Weekly	10	N
JMA	T319L60	0.1 hPa	F	1981–2010	Three per month	5	N
NCEP	T126L64	0.02 hPa	F	1999–2010	Daily	4	Y
UKMO	N216L85	85 km	O	1996–2015	Four per month	3	Y

Note. Reforecast types are either F (fixed) or O (on the fly). The CNR-ISAC model version is 20150326.

Centre National de Recherche Meteorologiques (CNRM), the National Centers for Environmental Prediction (NCEP), and the Met Office (UKMO), including the horizontal and vertical resolution of their atmosphere components, model tops, reforecast types, forecast periods, reforecast frequencies, ensemble sizes, and ocean components (or lack thereof). Among these models, 8 out of 10 are fully coupled Ocean and Atmosphere forecast systems, 2 are uncoupled (HMCR and ECCC), and 1 uses a slab ocean (ISAC). ECCC uses a persisted SST anomaly for the lower boundary condition.

These S2S models have very different representations of the stratosphere (Table 1): 3 out of 10 models (HMCR, BOM, ISAC) have relatively low model tops, with model top pressures greater than 10 hPa, while the rest have relatively high model tops.

2.2. The QBO Index

We use the zonal mean zonal wind anomaly at 50 hPa (U50) averaged between 10°S and 10°N to diagnose the QBO. This NOAA QBO U50 index, available at http://www.cpc.ncep.noaa.gov/data/indices/qbo.u50.index, is highly asymmetric in the easterly and westerly phases, with more samples in the westerly phase and fewer samples in the easterly phase. To account for this asymmetry, we composite MJO indices using the 33.3 and 66.7 percentiles of the QBO U50 index: if U50 is less than -2.37 m/s, it is considered the QBO easterly phase (EQBO), and if U50 is greater than 5.14 m/s, it is counted as the QBO westerly phase (WQBO). The results presented in this study are not sensitive to this particular choice of the QBO threshold values. For convenience, the MJO in the EQBO and WQBO will be referred to as MJO-EQBO and MJO-WQBO, respectively. This is justifiable because they differ significantly in amplitude, propagation speed, and period, as we shall see later.

2.3. The MJO Index

We use the real-time variant of the OLR-based MJO index developed by Kiladis et al. (2014) to diagnose MJO convection in the S2S models. The OMI index complements the popular Real-Time Multivariate MJO (RMM; Wheeler & Hendon, 2004) index for diagnosing the MJO activity. One advantage of OMI and ROMI is that, in addition to the MJO, these indices can track northward propagation of the intraseasonal convection in boreal summer, and hence are better suited for diagnosing the BSISO (Wang, Ma, et al., 2018). Wang, Sobel, et al. (2018) described the technical details to calculate the real-time OMI from reforecast data sets. They also showed that the S2S models exhibit prediction skill, measured by the bivariate correlation coefficient exceeding 0.6, ranging from ~15 to ~36 days in boreal winter. This is 5–10 days higher than the MJO circulation prediction skill based on the MJO RMM index, and the ROMI skill is systematically lower by 5 to 10 days in boreal summer than in winter. Interested readers may consult that paper for further details.

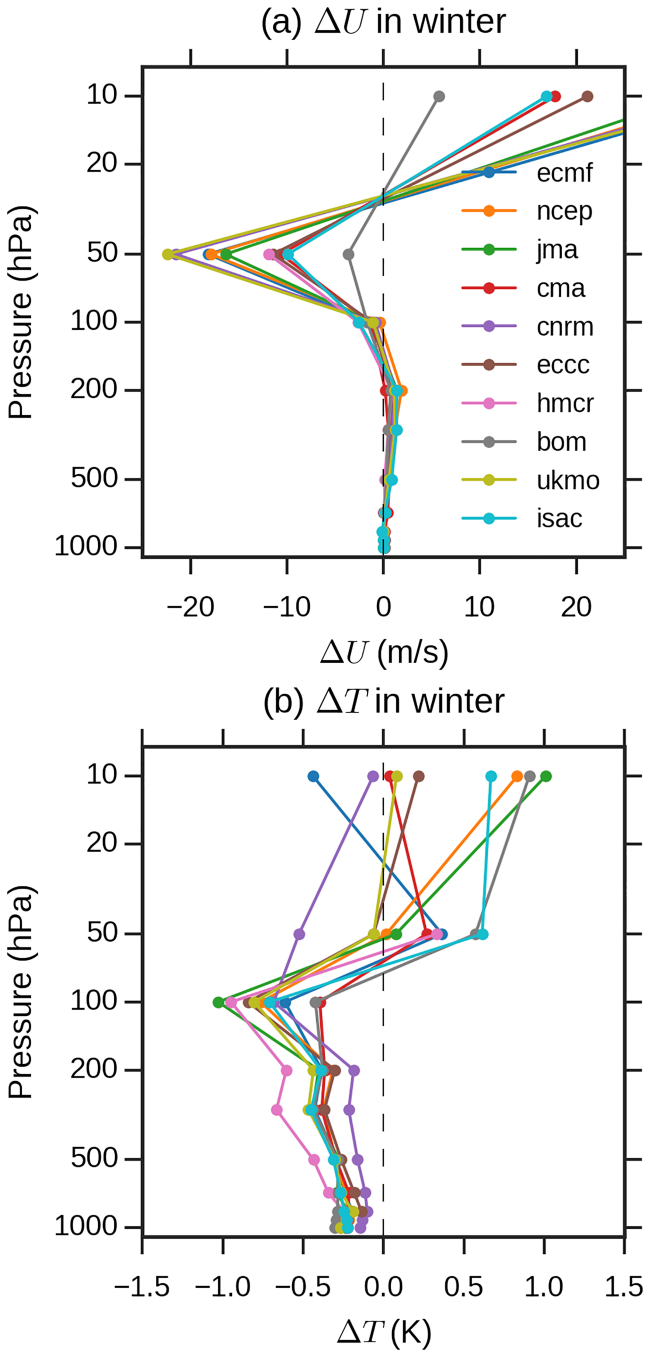

Figure 1. (top panel) Composite of difference in tropical zonal mean zonal winds during QBO easterly versus QBO westerly, ΔU, in boreal winter during the first 30 days of the S2S models. (bottom panel) Same as top panel but for zonal mean temperature.

2.4. A Linear Regression Model for the MJO Index

In addition to the S2S models, we adopt a simple statistical model to help understand the MJO-QBO relation in a model in which any QBO influence is only—at most—implicit via the MJO state. A linear lag-regression model is written in standard form as

$$\boldsymbol{y} = \boldsymbol{X}\boldsymbol{\beta} + \varepsilon,$$

where the predictand variables are $\boldsymbol{y} = [\mathrm{ROMI1}(t+\tau), \mathrm{ROMI2}(t+\tau)]^{\mathrm{T}}$ with forecast initial date t and forecast lead $\boldsymbol{\tau}$. The predictors are ROMI values at the initial date t and the previous day, $\boldsymbol{X} = [\mathrm{ROMI1}(t), \mathrm{ROMI2}(t), \mathrm{ROMI1}(t-1), \mathrm{ROMI2}(t-1), 1]^{\mathrm{T}}$, and $\boldsymbol{\varepsilon}$ is random noise. The regression coefficient $\boldsymbol{\beta}$ is computed as a function of forecast lead τ using the ROMI data from 1979 to 2016. Importantly, the regression coefficient does not vary with season or QBO phase. Jiang et al. (2008) and Kang and Kim (2010) showed that a similar simple linear regression model exhibits prediction skill for the MJO RMM index at lead times up to 15 days. This model will be referred to as the multiple linear regression (MLR) model throughout.

The MLR model is used to predict daily ROMI values during 1980–2016, with forecast lead times of 1 to 45 days and daily initialization to give the maximum possible sample size. We compute the forecast correlation skill for the MJO events with initial amplitude greater than 1. The MLR forecasts are computed using regression coefficients that are estimated from all the data, since our intent is not to estimate the practical skill of the MLR model, but rather to use the MLR model to help understand the QBO-MJO connection in a forecast model that has no explicit QBO dependence.

3. Results

3.1. The QBO in the S2S Models

The S2S models adopt distinct strategies for the initialization of the stratosphere, numerical schemes for gravity wave drag, and boundary conditions at the top of the atmosphere, all of which can potentially play important roles in maintaining the QBO circulation during the forecast periods. As a result, the QBO signatures in temperature and winds vary significantly across the S2S reforecasts. Figure 1 shows the EQBO minus WQBO difference in boreal winter zonal mean zonal wind (ΔU) and zonal mean temperature (ΔT), averaged between 10°S and 10°N on 10 pressure levels from 1999 to 2010. The QBO zonal wind difference, ΔU, at 50 hPa in the S2S models ranges from −5 m/s to greater than −20 m/s. The QBO temperature anomaly, ΔT, peaks at 100 hPa, and ranges from −0.3 to −1 K. Negative values of ΔT extend down to the lower troposphere. BOM (gray) shows the smallest differences in both ΔU and ΔT, perhaps because it has the lowest model top (10 hPa). Further inspection of these variables indicates that the QBO signatures decrease faster with forecast lead in some models than others, as shown in Figures S1 and S2 in the supporting information.

3.2. Impact of QBO on MJO Convection Prediction and Predictability in Boreal Winter

The bivariate correlation skill (COR) in boreal winter (December to March) from 1999 to 2010, a common period of the S2S data set, is computed for the 10 S2S models as

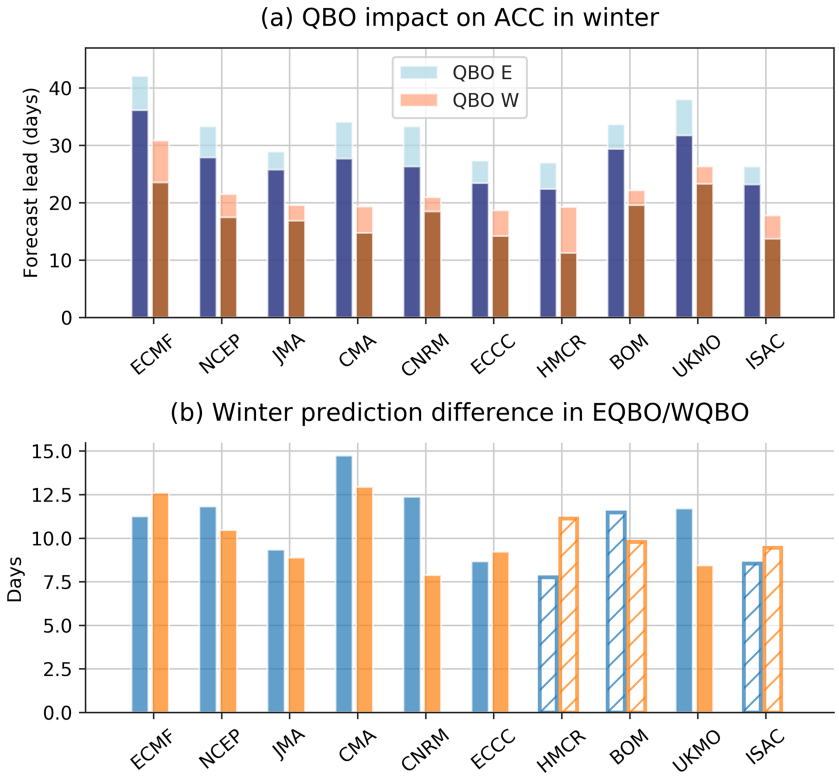

Figure 2. (a) Impact of the QBO on OMI prediction skill in winter using criteria ACC = 0.5 and 0.6 in boreal winter. (b) Difference in anomaly correlation skill between WQBO and EQBO in boreal winter 1999–2010. Blue and yellow: threshold values 0.5 and 0.6, respectively. Filled: modes with higher top (<5 hPa); empty: models with lower model top (≥5 hPa).

$$\mathrm{COR} = \frac{\sum_i F_{1,i}O_{1,i} + F_{2,i}O_{2,i}}{\sqrt{\sum_i F_{1,i}^2 + F_{2,i}^2}\sqrt{\sum_i O_{1,i}^2 + O_{2,i}^2}}$$

where *i* denotes the index of the (re)forecasts; F1 and F2 denote the ROMI1 and ROMI2 from the reforecasts, respectively; and O1 and O2 are ROMI1 and ROMI2 derived from observation. Model forecasts of the QBO are not used here, but will be tested in the next section. Figure 2a shows the correlation skill, using COR = 0.5 and 0.6 as threshold values, for all the S2S models in the two different QBO phases. The 10 S2S models unanimously show higher prediction skill in winter during EQBO; for example, the COR = 0.5 difference is ~11 days in the ECMWF and NCEP models. On average, the prediction skill difference between EQBO and WQBO is 11 days for COR = 0.5 and 10 days for COR = 0.6 (Figure 2b). There is no obvious relation between the ROMI prediction skill and prediction skill difference between WQBO and EQBO. Hence, the quantitative influence of the QBO appears to be independent of the MJO prediction in these S2S models.

Marshall et al. (2017) showed that for similar initial MJO amplitudes, the difference in the MJO RMM prediction skill between the two QBO phases in the BOM forecasts is unchanged for the reforecasts from the BOM model, but they were unable to rule out the influence of initial amplitude. On the other hand, it is possible that the MJO prediction skill may be sensitive to the amplitude of the forecast target at various lead times. We first test the initial amplitude dependence. Figures 3a and 3b show the ROMI correlation skill for the observed ROMI amplitude falling in the range 1.0–1.8 and >1.8 for two S2S models: ECMWF and NCEP, which yield relatively large sample size (~200–400). The ROMI correlation skill differs significantly in the two QBO phases for the two ranges. The difference in the prediction skill with initial amplitude 1.0–1.8 (solid curves) and stronger initial amplitude (>1.8) is weak, and marginal at best. We further test this dependence on the amplitude of ROMI at various forecast lead times: 0, 2, 4, ... , 24 days for the S2S models. Figures 3c and 3d show the ROMI correlation skill for the observed ROMI amplitude within the range 1.0–

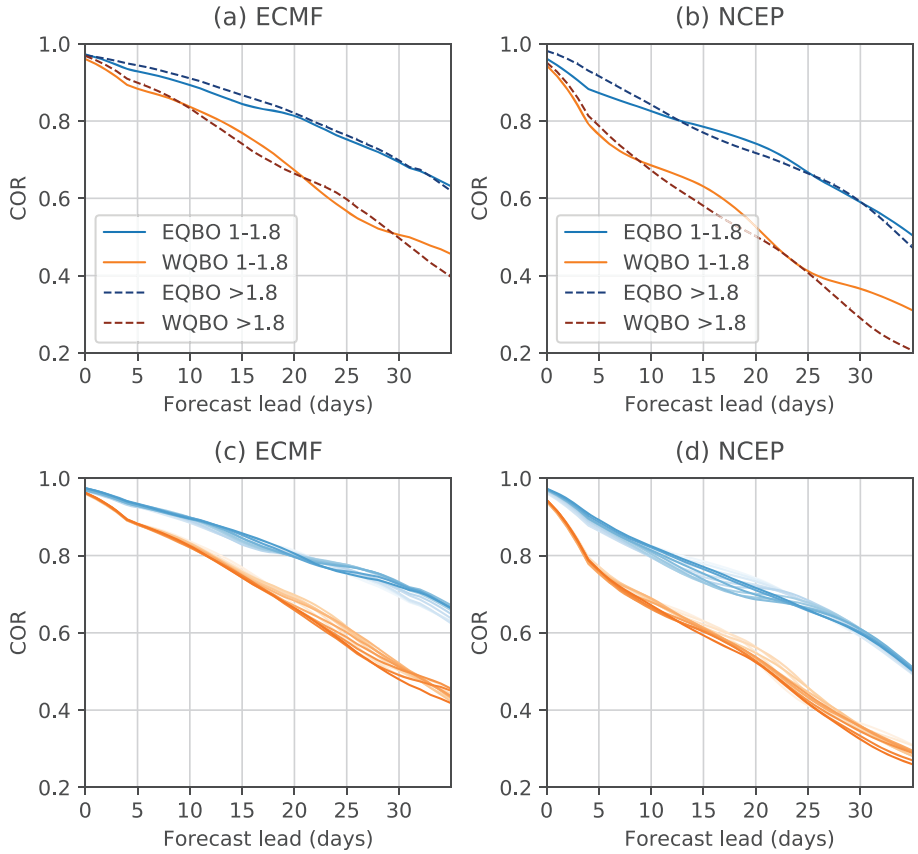

Figure 3. (top panels) Correlation skill for the reforecasts with initial amplitude falling into the range 1.0–1.8 (solid) and >1.8 (dashed) in the EQBO (blue) and WQBO (orange) for (a) ECMWF and (b) NCEP. (bottom panels) Same as top but for the initial/target amplitude range in the range 1.0–1.8 for (c) ECMWF) and (d) NCEP. Individual curves denote the composite with respect to the amplitude at various forecast lead days: 0, 2, 4, ... , 24. Light colors indicate small lead day composite; dark colors, longer lead composite.

1.8 for ECMWF and NCEP. The ROMI correlation skill differs significantly in the two QBO phases regardless of initial or target amplitude. Other S2S models show similar contrasts despite smaller sample sizes (<100). These results indicate that the amplitude of the ROMI does not play a role in the ROMI's prediction skill dependence on the QBO phases.

We further examine the predictability of the MJO in these ensemble prediction systems under different QBO phases using the quantity $T|_{SNR=1}$, which is defined to be the time at which the signal and noise variances are equal. The bivariate signal to noise ratio (*SNR*) is written as the ratio between the variance of the ensemble mean forecast and total variance:

$$\mathrm{SNR}(\tau) = \frac{\sigma_s^2}{\sigma_n^2}$$

The signal and noise of the ensemble forecasts are estimated as

$$\hat{\sigma}_s^2 = \frac{1}{N-1}\sum_{n=1}^{N}\sum_{p=1}^{2}\left(X_p^{-n} - X_p^{-}\right)^2,$$

$$\hat{\sigma}_n^2 = \frac{1}{N(E-1)}\sum_{n=1}^{N}\sum_{m=1}^{E}\sum_{p=1}^{2}\left(X_p^{nm} - X_p^{-n}\right)^2.$$

X_p denotes the OMI index, and the subscript p indicates its two principle components. N and E denote the number of forecasts and number of ensemble members, respectively. X^- is the overall mean, and X_p^{-n} denotes ensemble mean.

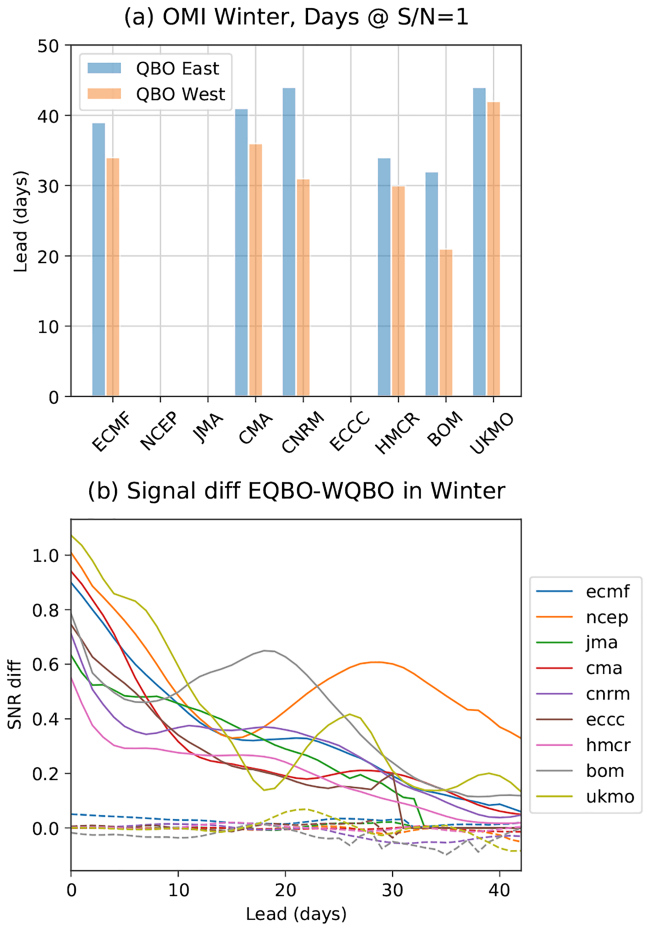

Figure 4. (a) Predictability measure using the time when signal to noise ratio (SNR) = 1. (b) Difference in signal $\widehat{\sigma}_s^2$ (solid) and noise $\widehat{\sigma}_n^2$ (dashed) between EQBO and WQBO.

SNR does not decrease to 1 by the end of their forecast in several models (NCEP, JMA, ECCC) due to underdispersiveness. Figure 4a shows $T|_{SNR\ =\ 1}$ for the remaining six ensemble prediction models. All these models show higher predictability for MJO-EQBO during winter, consistent with our analysis of COR. Specifically, $T|_{SNR\ =\ 1}$ in the six models is consistently larger for MJO-EQBO than in MJO-WQBO by 1–11 days, depending on the model. BOM shows the largest difference (11 days), ECMWF shows a difference of 7 days, while the difference for UKMO is 1 day. As with prediction skill, there appears to be no relationship between the MJO predictability and its dependence on the QBO. Figure 4b indicates that the increase in predictability in EQBO may be attributed to higher $\widehat{\sigma}_s^2$ (solid), since $\widehat{\sigma}_n^2$ (dashed) shows no appreciable change in the two QBO phases.

Another measure of predictability that is closely related to the signal-to-noise ratio described above for ensemble prediction is potential predictability. Potential predictability is defined by taking one of the ensemble members as the truth, assuming that the forecast model is perfect, and verifying forecasts against it. Figure 5a shows that potential predictability in EQBO is notably higher than in WQBO in eight out of nine S2S models (excluding ISAC, which has one member), although the difference between the two QBO phases is quantitatively smaller than that in prediction skill (cf. Figure 2). With these metrics, we can re-examine the initial amplitude dependence; here we do so by selecting reforecast cases with the same initial amplitude range (1.0–1.6) in the ECMWF model. Here the initial amplitude is calculated from the forecast ensemble member chosen for verification (not from observation as elsewhere). Figure 5b shows that for the similar initial amplitudes, a larger amplitude is maintained in MJO-EQBO than in MJO-WQBO for all the leads in both forecasts and observations, and the potential predictability (Figure 5c) is notably higher in EQBO as well. The MJO-WQBO cases weaken more than in the MJO-EQBO cases at longer leads in this model, which likely causes decreased skill of MJO-WQBO but is accounted for in potential predictability. To further test the initial amplitude dependence, we select the WQBO cases in a slightly higher amplitude range in verification (1.1–1.7), as the initial amplitude in forecasts is more comparable between MJO-EQBO with initial amplitude (1.0–1.6) and MJO-WQBO (1.1–1.7). In this case as well, the potential predictability does not improve in MJO-WQBO. This indicates that we may rule out the initial amplitude as the primary influence on potential predictability.

3.3. Stratospheric Conditions Versus Initial Conditions/Persistence

Having established that the QBO state is strongly associated with variations in the skill of MJO prediction in the S2S models, one may ask if the QBO state predicted by each model is truly a causal factor influencing MJO prediction skill in that model. An alternative hypothesis would be that the QBO influence is simply a consequence of the initial conditions, since those are taken from observations in which the QBO-MJO relationship is already present. Another alternative hypothesis would be that the MJO is more inherently predictable—for example, more autocorrelated with itself over time—in EQBO than WQBO years, so that even if there were no difference in the model forecasts between QBO phases, they could show greater skill in EQBO than WQBO because they are being compared to more predictable observations in EQBO.

The S2S models rely on both boundary conditions and initial conditions to make informative and skillful forecasts. The lower stratosphere, though not a boundary condition per se, may in some sense function as one from the perspective of tropospheric weather. The S2S forecast models have very different lower stratosphere characteristics due to variations in numerics and physics (Table 1). The majority of the models have relatively high model tops, but 3 of the 10 models (BOM, ISAC, and HMCR) have model tops at 5 hPa or lower (in altitude; higher in pressure). The high-top models have slightly higher mean MJO prediction skill difference (~11 days for the threshold value COR = 0.5, ~10 days for COR = 0.6) than the low top models (~9, ~10

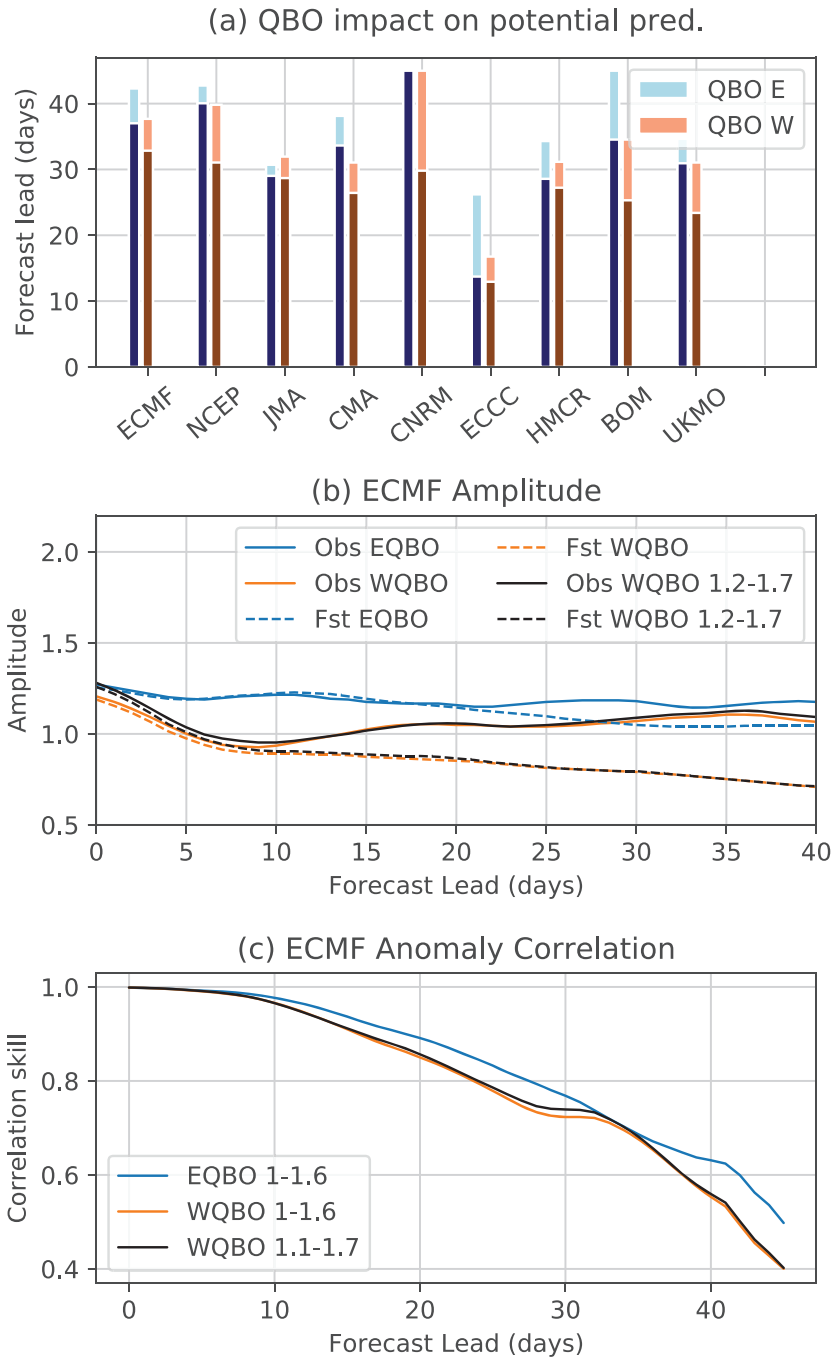

Figure 5. (a) Potential predictability. (b) Composite of amplitude in observations (solid) and reforecasts (dashed) from ECMWF with initial amplitude within the range 1–1.6 for EQBO and WQBO, and for WQBO (1.1–1.7). (c) Correlation skill for ECMWF for EQBO (1–1.6), WQBO (1–1.6), and WQBO (1.1–1.7).

days for COR = 0.6**)** in winter (Figure 2b). To further explore the QBO's influence on MJO skill, one may attempt to correlate models' skill difference during EQBO and WQBO with various QBO signatures, for example, temperature or temperature stratification at 100 hPa, which seems to define the most likely physical pathway for the MJO-QBO connection (e.g., Densmore et al., 2019; Martin et al., 2019; Hendon & Abhik 2018; Lee & Klingaman 2018; Nishimoto & Yoden, 2017; Son et al., 2017). This analysis does not yield any statistically significant relationship, however. This is perhaps unsurprising given that the sample

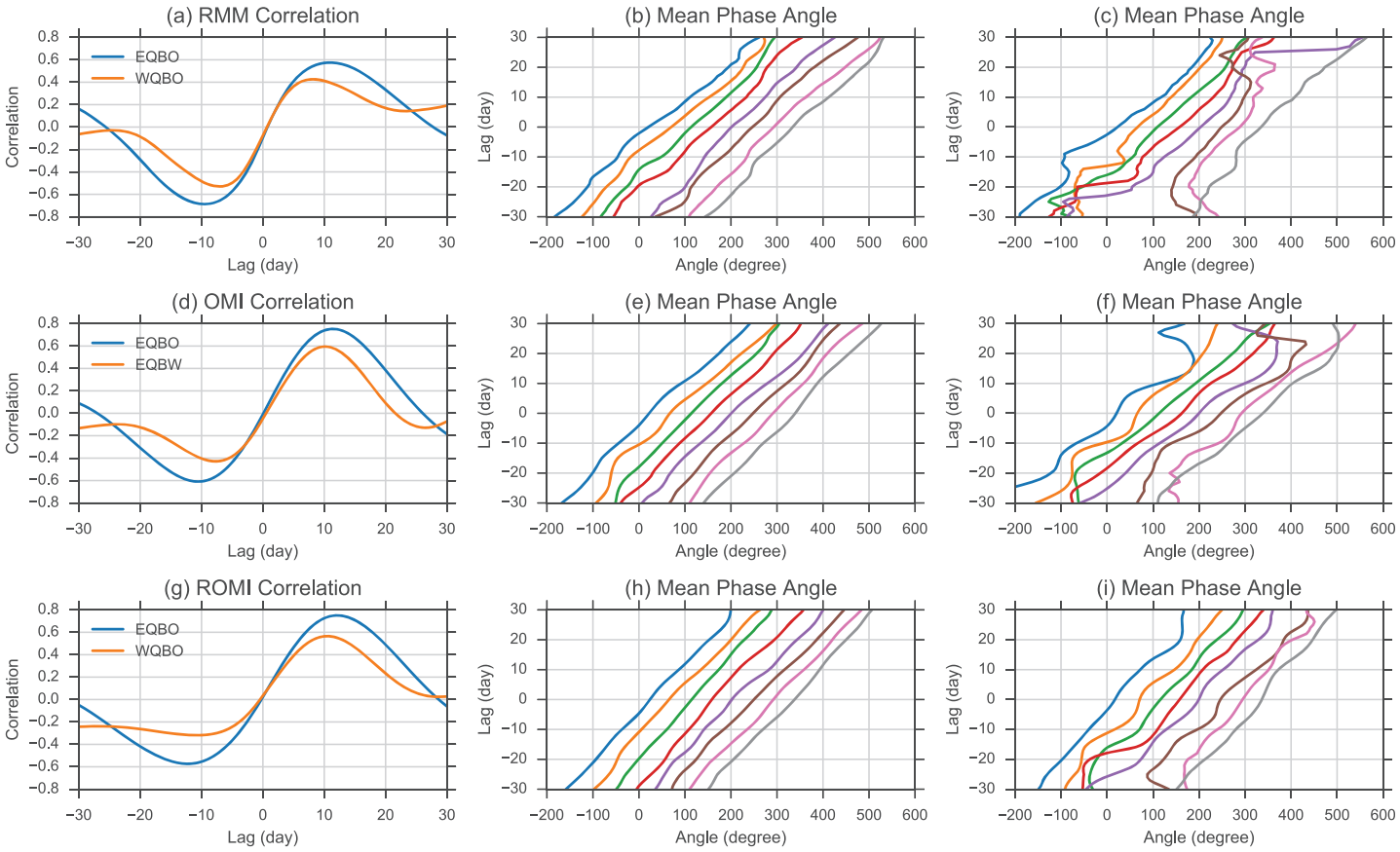

Figure 6. (top row, a) Correlations between PC1 and PC2 for RMM in EQBO and WQBO in boreal winter. (b) Composites of mean phase angles in EQBO. (c) Same as in (b) but in WQBO. (middle row) Same as top row but for OMI. (bottom row) Same as top row but for ROMI. Differently colored curves in the middle and rightmost panels indicate eight different MJO phases.

size is less than 10 (see Figure S4), but nonetheless is consistent with the view that the model-predicted QBO has a weak influence on MJO prediction skill.

On the other hand, one may argue that, if the influence of the predicted QBO state on MJO evolution were maintained in each model through the forecast—as opposed to entering only through the initial conditions—then the difference in noise estimates ($\widehat{\sigma}_n^2$) between the two QBO phases would be significant. However, as shown in Figure 3b this is not the case: instead, the difference in the signal estimates ($\widehat{\sigma}_s^2$) in two QBO phases is robust across the S2S models, suggesting that the difference in prediction skill and predictability shown above comes from the initial conditions or persistence. In the following, we will present further evidence supporting this hypothesis.

Figures 6a, 6d, and 6g show the lag correlation between the two principal component time series (PC1 and PC2) for three MJO indices: RMM, OMI, and ROMI, during the winter season (December to March) from 1980 to 2000. All indices have higher peak values around day 10 in EQBO than in WQBO. The period implied by the days between the maximum value at positive leads and the minimum at the negative leads is also longer in EQBO than in WQBO by a few days.

We next examine the mean phase angle Θ, defined as

$$\Theta = arctan\left(\frac{1}{N}\sum_i \sin\theta_i, \frac{1}{N}\sum_i \cos\theta_i\right),$$

where θ is the phase angle between the PC1 and PC2 components of the ROMI index. The composites of the mean phase angle (Wang, Ma, et al., 2018,Wang, Sobel, et al., 2018) in EQBO and WQBO in the middle and

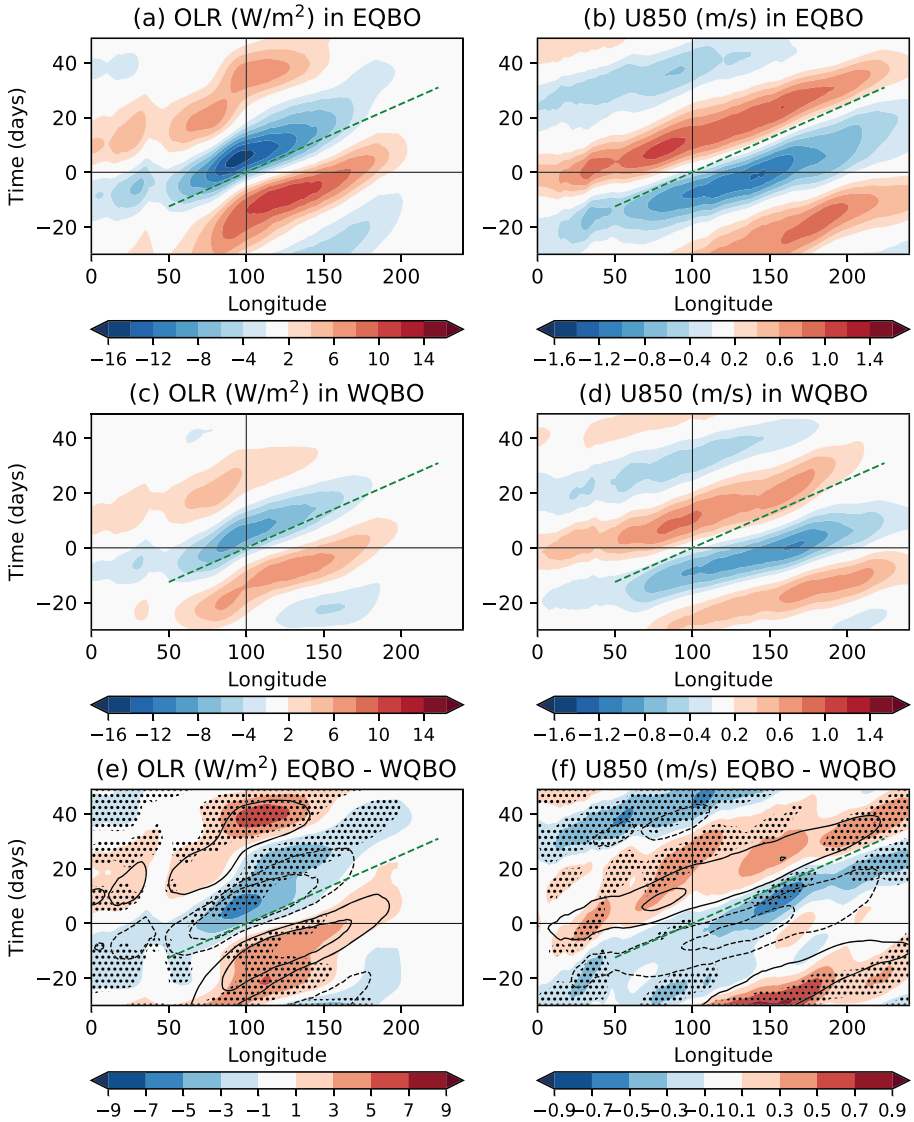

Figure 7. (left column, a) Composite of OMI reconstructed OLR anomalies in EQBO from December to March. (c) as Same as (a) but for WQBO. (e) Difference in OLR anomalies between EQBO (a) and WQBO (c). Stripes indicate that the difference is statistically significant at 95% using a Student's *t* test. Green dashed lines indicate a propagation speed of 5 m/s. (right column) Same as in the left column but for the zonal mean zonal wind at 850 hPa.

right columns of Figure 6 further break down the phase propagation into 8 phases. The mean phase angle is noisier in MJO-WQBO than in MJO-EQBO, propagating with near constant phase speed in the latter. The lag correlation and phase composite together indicate that the observed MJO indices are inherently more regular and less noisy in EQBO than in WQBO, consistent with the greater predictability in EQBO shown above.

The difference in the MJO indices as shown above reflects changes in the MJO's dynamical structures in the two QBO phases. To illustrate this point, we composite the reconstructed OLR from the OMI index upon the QBO. The MJO events are selected from 1979 to 2016, based on the following criteria: (1) OMI is in phase 3 or 4 at day 0 such that the convection is located around Maritime Continent, (2) the OMI amplitude is greater than 0.5 at day 0, and (3) any two selected events must be separated by at least 30 days to prevent double-counting. Using the same QBO index and criteria (−2.37 and 5.23 m/s) for QBO phases, this leads to 29 MJO-EQBO events, and 31 MJO-WQBO events in 1979–2016. The results described below are not sensitive to the period. The reconstructed OLR anomalies R are computed as

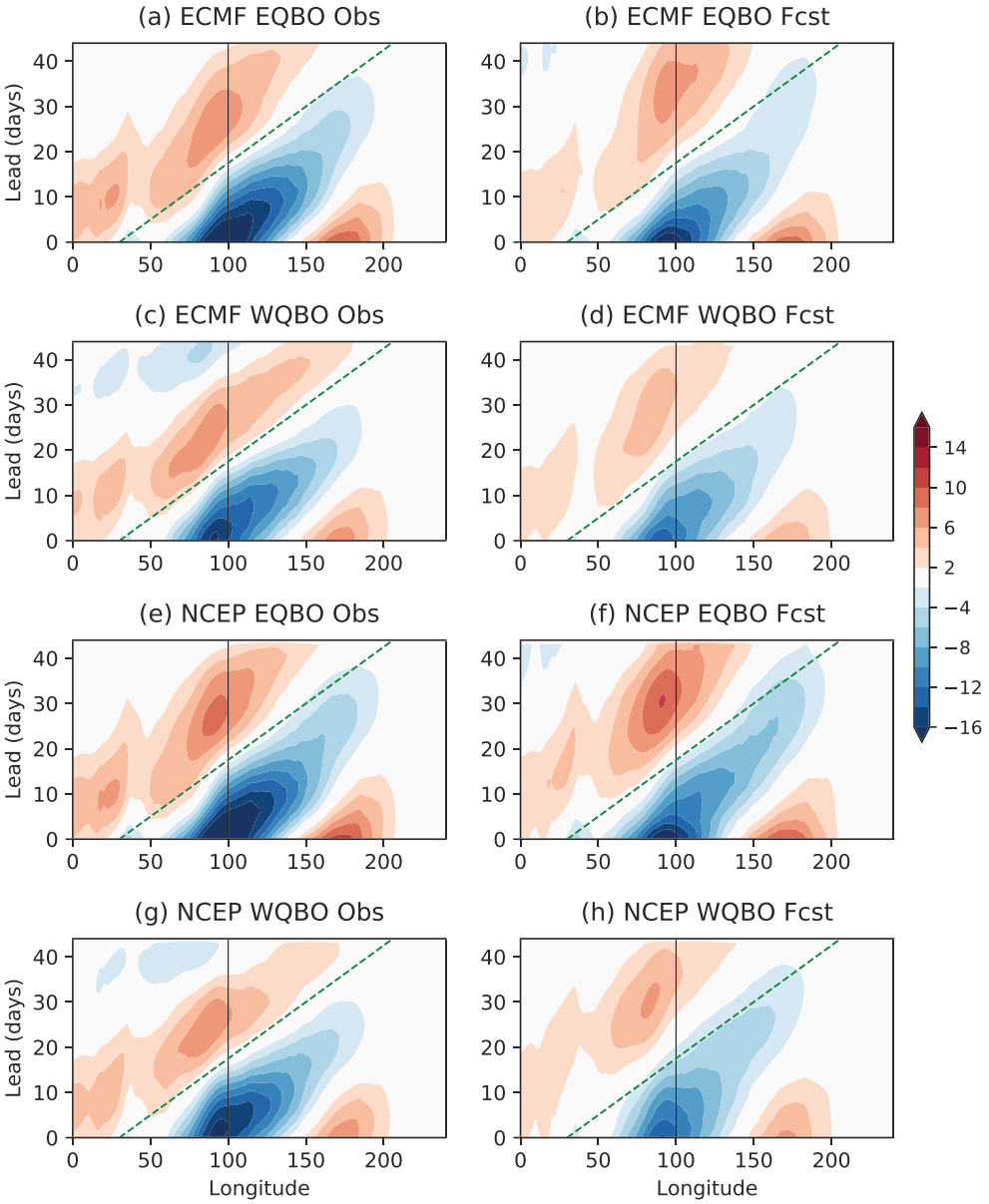

Figure 8. ROMI reconstructed OLR anomalies (W/m^2) averaged 20°S–20°N from ECMWF and NCEP models in EQBO and WQBO. (left panels) Verifications. (right panels) Forecasts. Green dashed lines indicate a propagation speed of 5 m/s.

$$R(x,y,t) = \mathrm{PC1(t)}\times\mathrm{EOF1}(x,y,doy) + \mathrm{PC1(t)}\times\mathrm{EOF1}(x,y,doy),$$

where PCs are the principle component time series, EOFs are the empirical orthogonal functions, and *doy* denotes day of year.

Figure 7 shows the lag composites of the reconstructed OLR and zonal wind at 850 hPa (U850) anomalies with respect to the initial MJO phase 4 in the two QBO phases during the extended boreal winter season (December to March). The MJO OLR anomalies are notably stronger in EQBO (Figure 7a) than in WQBO (Figure 7c), and the difference in the OLR anomalies between EQBO and WQBO is statistically significant based on a Student's *t* test at 95% level (Figure 7e). The period at 100°E is ~5–10 days longer in EQBO than in WQBO in both OLR and U850. Correspondingly, the phase speed of MJO-EQBO is notably slower, as also shown in Figure 3 of Zhang and Zhang (2018) for precipitation. The structural difference is robust in 850-hPa zonal wind (Figures 7b and 7d), and also in different MJO phases at day 0 or if different indices are used. This

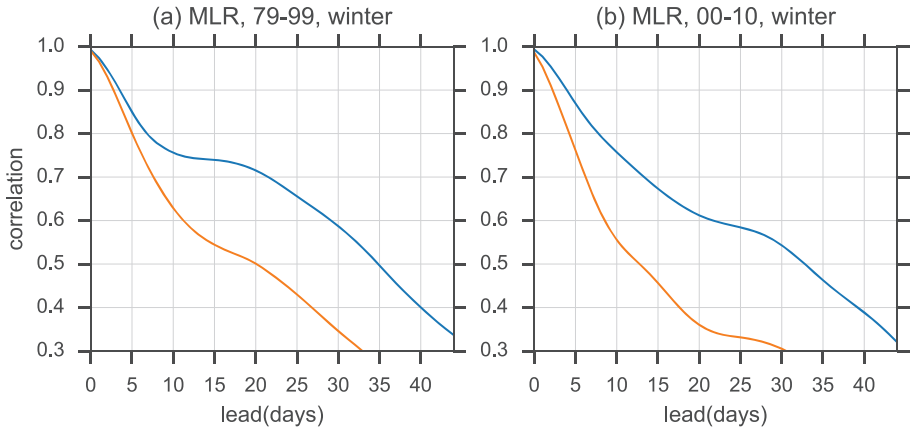

Figure 9. Correlation between the fitted PCs by the MLR and observation in boreal winter during (a) 1979–1999 in the left panel and (b) 2000–2010 in the right panel, the common period for the S2S models. Blue curve: MJO-EQBO. Orange curve: MJO-WQBO.

suggests that the MJO-EQBO and MJO-WQBO exhibit different spectral properties within the broad intraseasonal band: MJO-EQBO is stronger, propagates slower, and has longer period than MJO-WQBO.

Now we proceed to analyze the structural difference between the MJO-EQBO and MJO-WQBO in reforecasts. Similar to the composite analysis for observations in Figure 7, the right panels of Figure 8 show the reconstructed OLR anomalies from the predicted ROMI initialized at phases 3 and 4 with initial amplitude greater than 1 for the ECMWF and NCEP models. The verifications differ for each model because of differences in the initialization times, and are also shown in the left panels. As Figure 7, the verifications in the two models show that MJO-EQBO is slower and stronger than MJO-WQBO. The MJO-EQBO in forecasts is slower and stronger, and comparable to the verification except for the biases at longer leads. But MJO-WQBO (Figures 8d and 8h) in the forecasts is notably slower than in the verification, which might contribute to the skill reduction in WQBO. The contrast between the two is weaker in forecasts than in observations. This suggests that potential predictability, computed by verifying against one ensemble member from each forecast model, rather than against observations (Figure 3), should also display a difference between MJO-EQBO and MJO-WQBO. Indeed, this is what was demonstrated in Figure 4. The structural difference between MJO-EQBO and MJO-WQBO in reforecasts can also be identified from the ROMI values. The correlation between ROMI1 and ROMI2 in forecasts for all the models (Figure S5) shows higher peak values in MJO-EQBO than in MJO-WQBO.

Next, we test the influence of the QBO in the MLR model. We compute the correlation between the MLR-predicted ROMI values and the observations in the same manner as we computed that between the S2S reforecasts and observations. Figure 9 shows that the MLR prediction skill in EQBO and WQBO differ by more than 10 days using the threshold COR = 0.5; this is true both from 2000 to 2010 (Figure 9b), and similarly during 1979–1999 (Figure 9a). This large difference is quantitatively consistent with the S2S model results (Figure 2b). However, as discussed in section 2.4, the MLR coefficients are independent of the QBO phase. The MLR model prediction is based only on the state of MJO on the initial and previous days, and uses no explicit information about the state of the stratosphere (or anything else other than the OMI index). As a result, the MLR model is agnostic to the explicit QBO phase. Despite this, the fact that MLR still captures the QBO influence on the MJO prediction skill indicates that the QBO influence is implicitly included in the initial conditions of the MLR model and in the verifying observations. The results also confirm the findings from Marshall et al. (2017) and Lim et al. (2019) that the association between the stratospheric QBO state and MJO predictability is present in a statistical model that lacks explicit knowledge of the stratosphere.

Taken together, our results lead us to several inferences. First the MJO prediction is strongly dependent on the observed QBO state, but weakly dependent on the QBO state in the S2S forecasts. Second, the EQBO-WQBO differences in both potential predictability and signal-to-noise ratio indicate that differences in MJO persistence in the target observations cannot be the sole factor responsible for the differences in real

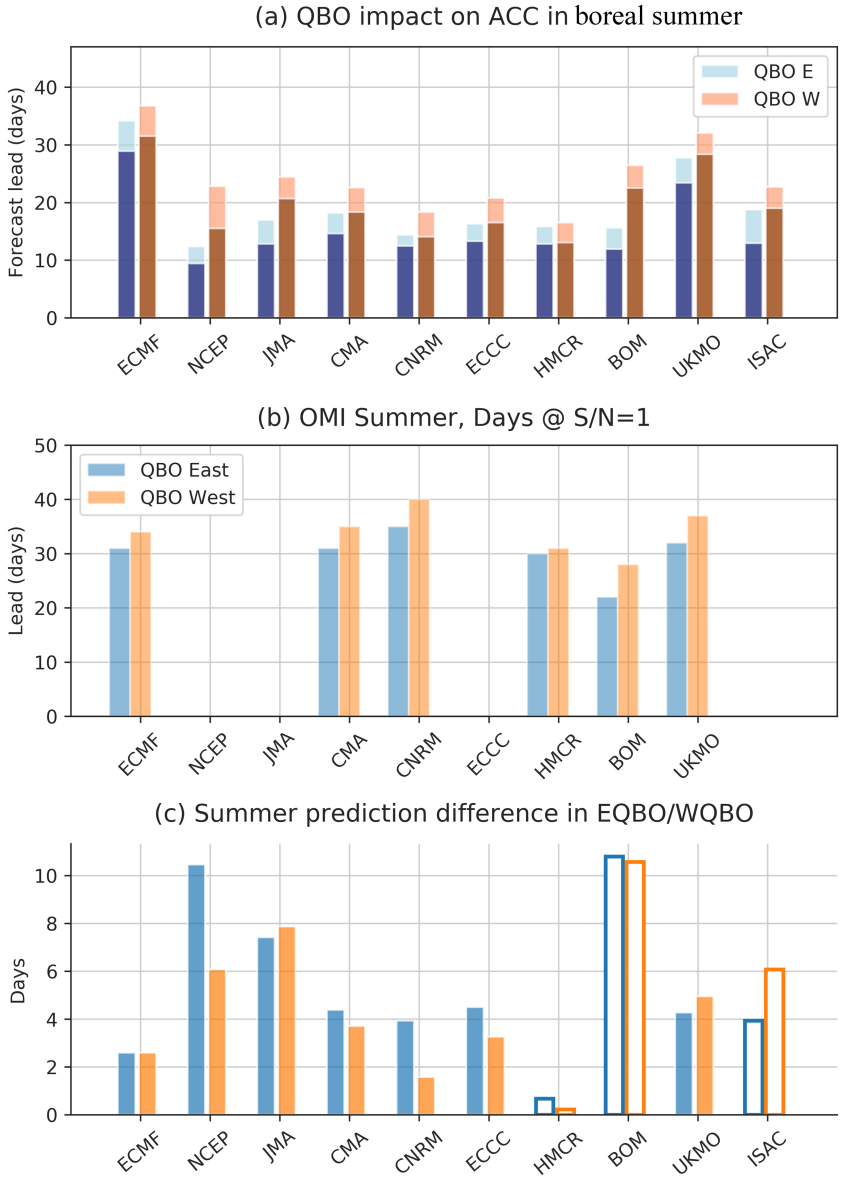

Figure 10. (a) Impact of QBO on the OMI prediction skill using criteria ACC = 0.5 and 0.6 in boreal summer. (b) Predictability measure using the time when SNR (signal to noise ratio) = 1. (c) Difference in anomaly correlation skill between WQBO and EQBO in boreal summer 1999–2010. Blue and yellow: threshold values 0.5 and 0.6, respectively. Filled: models with higher tops (<5 hPa); empty: models with lower model tops (≥5 hPa).

prediction skill, since the target observations are not used in computing these measures. Third, the observed MJO index is less noisy and more regular in EQBO than WQBO, and the MLR shows better skill during EQBO as well, even though it contains no information about the stratosphere. These facts suggest that, the previous inference notwithstanding, more regular propagation of the tropospheric MJO during EQBO versus WQBO is at least part of the explanation for the increased actual prediction skill in EQBO versus WQBO.

These inferences collectively lead us to the broader conclusion that differences in the forecast QBO in the models are not the main factor contributing to the MJO skill difference between EQBO and WQBO. Rather, EQBO-WQBO differences in both initial conditions and the target observations used for verification appear to play roles. The relevant differences in initial conditions, however, cannot simply be differences in amplitude, since controlling for amplitude does not eliminate the differences in prediction skill. What

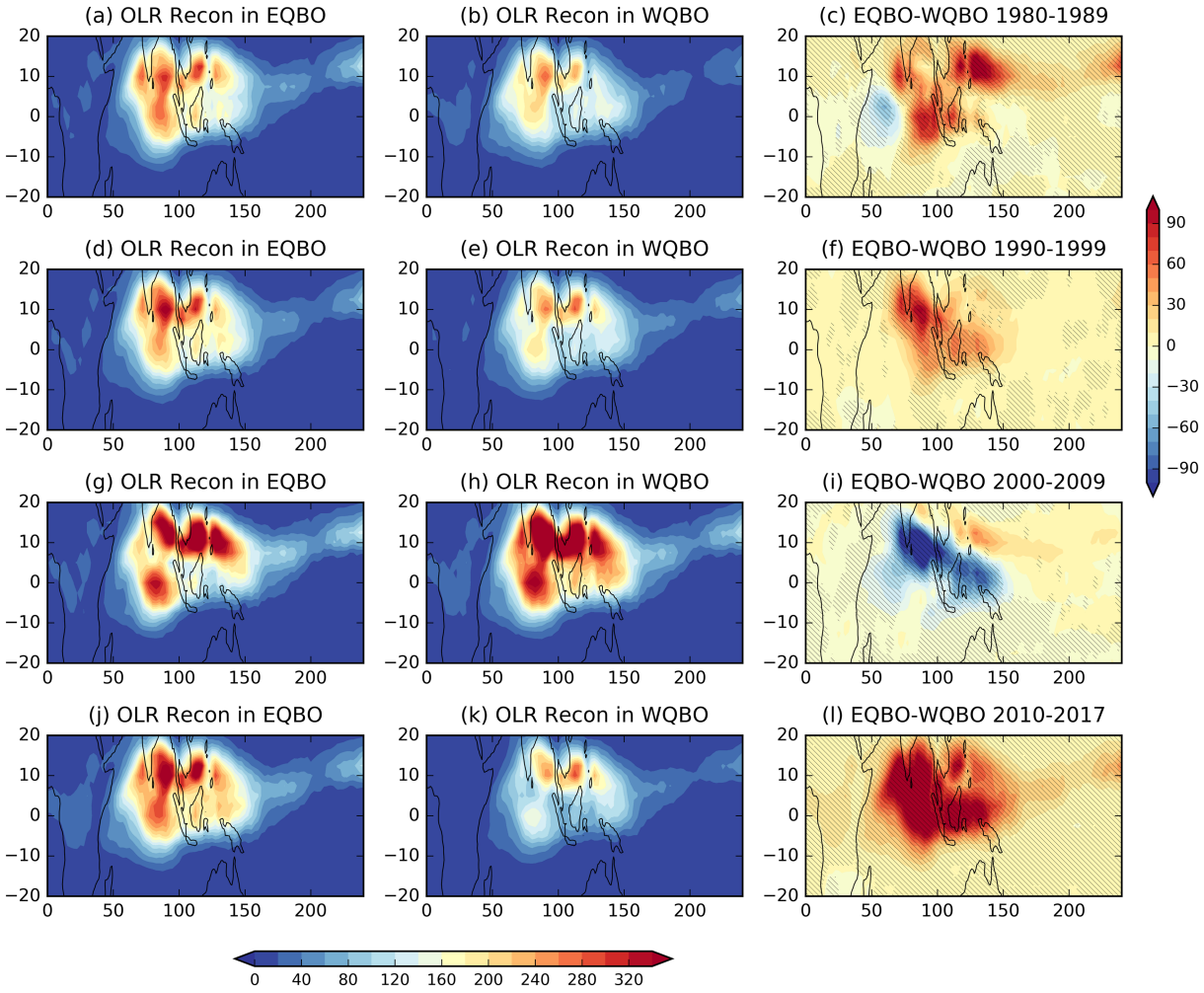

Figure 11. Variance of reconstructed OLR anomalies (W^2/m^4) from the OMI index in the summer season (July to September) in 4 decades under QBO (left column) easterly and (middle column) westerly phases, and (rightmost column) the difference in the two QBO phases. Hatching in the rightmost column indicates where the differences in variances are statistically significant at 95% percent level from Levene's test.

structural differences in the MJO are important and how those are manifest in the initial conditions is a topic for future research.

3.4. Impact of QBO on BSISO Prediction Skill in Boreal Summer

The above discussion focuses on the QBO influence on MJO predictions in boreal winter. We explore the analogous relation for the boreal summer intraseasonal oscillation (BSISO). Figures 10a and 10b show COR in boreal summer (June–September) during 1999–2010. In many S2S models, COR is higher by ~10 days under WQBO than EQBO using either COR = 0.5 or 0.6 as a threshold. This is in stark contrast with the QBO-MJO prediction skill relationship in winter, and is unexpected. Yoo and Son (2016) found no linear correlation between QBO and MJO-OMI amplitude in summer, in contrast to winter from 1979 to 2012. However, most S2S models only have limited reforecast periods, and here they are compared over the common period in 1999–2010. As will be discussed below, a consistent relation between QBO and MJO-OMI amplitude in summer is indeed present in observations during this period. One might speculate that this BSISO-QBO relationship is a result of tropical sea surface temperature changes related to the El Niño–Southern Oscillation (ENSO) phenomenon, rather than of the QBO influence. For example, Liu et al. (2016) have shown that ENSO modulates northwestward propagating intraseasonal oscillations in boreal summer, but these are not the eastward and northward propagating BSISO signals that are represented by the OMI/ROMI index. The same skill assessment (Figure 10) is re-computed in the ENSO neutral years,

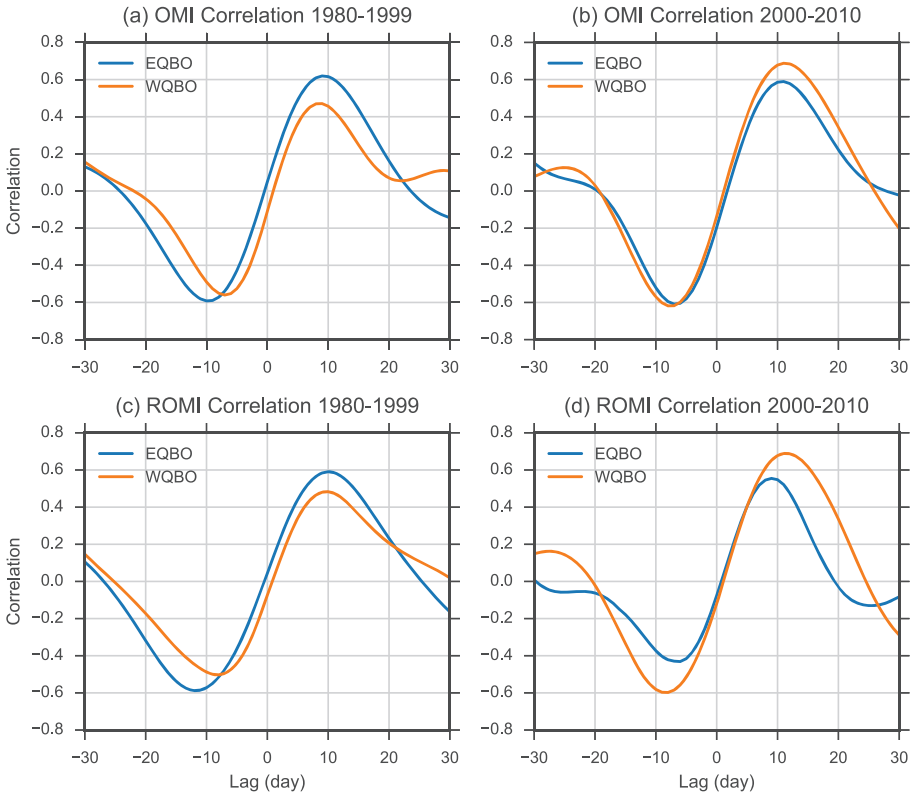

Figure 12. (a) Lag correlations between PC1 and PC2 for OMI in EQBO and WQBO in boreal winter from 1980 to 1999. (b) Same as in (a) but for 2000–2010. (c and d) Same as in (a) and (b) but for ROMI.

and the skill difference in the two QBO phases are overall robust, suggesting that ENSO may not be a dominant player in the BSISO-QBO relationship.

To examine this relationship further, we composite the OMI reconstructed OLR anomalies on the QBO phases in boreal summer (May to October) in the recent four decades: 1980–1989, 1990–1999, 2000–2009, and 2010–2017. Figure 11 shows the variances of the reconstructed OLR anomalies in WQBO, EQBO, and the difference between these two QBO phases. The maximum variances are located over the eastern equatorial Indian Ocean, Bay of Bengal, South China Sea, and northwest western tropical Pacific Ocean in both QBO phases. These patterns are consistent with those found in prior studies (e.g., Lawrence & Webster, 2002; Sobel et al., 2010). The difference in OLR intraseasonal variance between the two QBO phases is shown in the rightmost column of Figure 11 for each of the past four decades. The variance under EQBO (leftmost column) does not seem to have any strong decadal variations during the past 4 decades. However, the variance in WQBO (middle column) is particularly strong in 2000–2009, compared to the other decades. The difference in variance (indicated by hatching) is statistically significant at the 95% level in most areas using Levene's test (Levene, 1960). Hence, the QBO influence on intraseasonal convection is at times reversed in the boreal summer: the BSISO convection is reduced in amplitude during EQBO in 2000–2009, in contrast to its strengthening in the other three decades. A similar composite analysis was also performed for boreal winter, and in that case we do not see a change in the QBO-MJO relationship from one decade to the next since 1979.

The lag correlations of the PC 1 and 2 for ROMI are useful indicator for the predictability of ROMI (Figure 6). Here, we show that lag correlations in summer also change in the two periods: 1980–1999 and 2000–2010 (Figure 12). The OMI and ROMI are notably less noisy and more coherent for WQBO, and have higher peak correlation coefficient in 2000–2010 (Figures 12b and 12d), suggesting that ROMI is more predictable in the QBO westerly phase. This is consistent with the model forecast verification (Figure 10). On the other hand, the lag correlation of OMI and ROMI during the period 1980–2000 (Figures 12a and 12c) shows the opposite relationship: its peaks in absolute value are larger in EQBO than in WQBO.

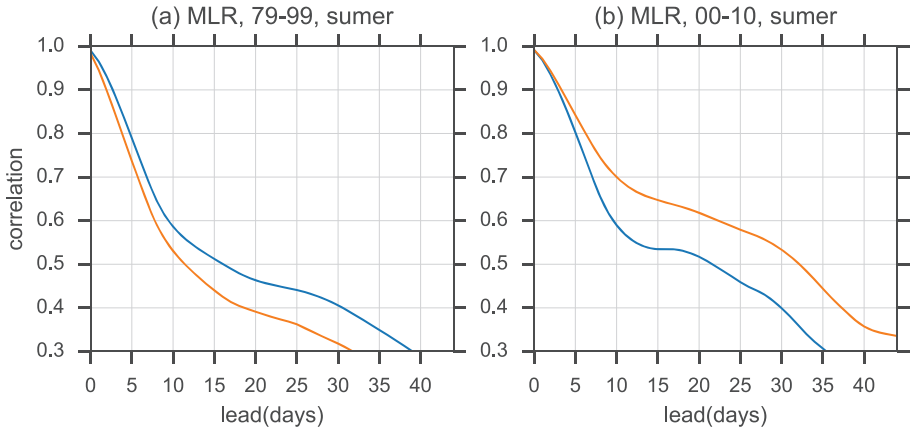

Figure 13. Correlation between the fitted PCs by the MLR and observation in boreal summer during (a) 1979–1999 and (b) 2000–2010, the common period for the S2S models. Blue curve: EQBO. Orange curve: WQBO.

The above analysis strongly suggests that the QBO influence on ROMI prediction skill during summer should also exhibit decadal variability. However, this is difficult to evaluate using the S2S models, as most of the S2S models have limited reforecast periods that do not extend back to 1980. To further explore this hypothesis, we examine the QBO influence on BSISO prediction using the MLR model. The MLR correlation skill is estimated during two different periods, 1979–1999 and 2000–2010, to examine QBO influences on the BSISO prediction skill over these time periods of interest.

Figure 13 shows that this simple statistical model has skill extending to 19 days using the threshold bivariate correlation = 0.5. This skill is lower than that of most S2S models in summer (Figure 13). We calculate the COR for two periods: 1979 to 1999 and 2000 to 2010. Figures 13a and 13b show that the summer COR from the MLR model is higher under WQBO during 1999 to 2010, similar to the S2S models (Figure 10b). But this relationship reverses during 1979 to 2000. The opposite impact QBO on summer bivariate correlation skill is also consistent with the composite of the OLR anomalies discussed above.

4. Conclusions

We have examined the impact of the stratospheric QBO on the skill with which the WMO Subseasonal to Seasonal forecast models predict tropical intraseasonal convection, as represented by the real-time OLR MJO index (ROMI). Although some S2S models do not have well-resolved stratospheres because of relatively low model tops, the stratospheric QBO nevertheless has a strong relationship with ROMI prediction skill across the ensemble of S2S models. The skill during boreal winter is higher in the QBO easterly phase (EQBO) than the westerly phase (WQBO) in all 10 models by ~10 days, using the anomaly correlation coefficient 0.5 as a criterion during 1999–2010; this difference between QBO phases is independent of the differences in MJO prediction skill across the individual models. In contrast, the skill in boreal summer decreases in EQBO during this period. It is further shown that there is also a close relationship between the QBO and BSISO, but that this relationship varies over the past several decades, with a stronger BSISO during the QBO westerly phase during the first decade of the twenty-first century and a stronger BSISO under EQBO during other periods.

Analysis of the observations indicates that during winter, several different MJO indices (OMI, ROMI, RMM) are inherently less noisy and hence more predictable in EQBO than WQBO. Potential predictability analysis shows qualitatively similar but smaller contrast between the two QBO phases, indicating that the QBO dependence of actual prediction skill is not solely due to the verifying observations. Compositing the MJO OLR anomalies upon QBO phases shows that the MJO-EQBO is stronger, has a longer period, and propagates more slowly. Further, a simple regression model also exhibits greater skill during EQBO than during WQBO, even though it does not contain any explicit information about the stratosphere.

Taken together, these results suggest that the relationship between QBO phase and MJO prediction skill in northern winter is a consequence of EQBO-WQBO differences in the initial conditions (though not solely in

amplitude), in the persistence of the MJO in the verifying observations, or—most likely—some combination of the two, but not of an actual stratospheric influence exerted on the tropospheric MJO within the model simulations.

While our analysis strongly suggests that the stratosphere is not crucial for the prediction of the MJO under the influence of the QBO, our results do not disprove the general notion that stratosphere-troposphere coupling is important for tropospheric weather. In contrast, our analysis illustrates the added complexity in the predictability problems that involve initial conditions, forecast verification, and dynamical coupling between troposphere and other components of the Earth systems, that is, stratosphere, ocean, and land.

Acknowledgments
This research has been conducted as part of the NOAA MAPP S2S Prediction Task Force and supported by NOAA grant NA16OAR4310076. S.W. and A. H.S. also acknowledge support from NSF AGS-1543932 and ONR N00014-16-1-3073. We are grateful for the insightful comments by three anonymous reviewers. We thank Haibo Liu for obtaining and organizing the S2S data set from the ECMWF data portal. The S2S reforecast data set is available at http://apps.ecmwf.int/datasets/data/s2s-reforecasts-instantaneous-accum-ecmf/levtype=sfc/type=cf/ and https://iridl.ldeo.columbia.edu/SOURCES/.ECMWF/.S2S. The QBO index is available through http://www.cpc.ncep.noaa.gov/data/indices/qbo.u50.index. The ROMI index from 1979 to 2018 and the S2S ROMI data are available at https://github.com/wangsg2526/ROMI or upon request from the first author.

References

Baldwin, M. P., Gray, L. J., Dunkerton, T. J., Hamilton, K., Haynes, P. H., Randel, W. J., et al. (2001). The quasi-biennial oscillation. *Reviews of Geophysics*, *39*(2), 179–229.

DeMott, C. A., Klingaman, N. P., & Woolnough, S. J. (2015). Atmosphere-ocean coupled processes in the Madden-Julian oscillation. *Reviews of Geophysics*, *53*, 1099–1154. https://doi.org/10.1002/2014RG000478

Densmore, C. R., Sanabia, E. R., & Barrett, B. S. (2019). QBO Influence on MJO Amplitude over the Maritime Continent: Physical Mechanisms and Seasonality. *Monthly Weather Review*, *147*(1), 389–406. https://doi.org/10.1175/MWR-D-18-0158.1

Hendon, H. H., & Abhik, S. (2018). Differences in vertical structure of the Madden-Julian Oscillation associated with the quasi-biennial oscillation. *Geophysical Research Letters*, *45*(9), 4419–4428. https://doi.org/10.1029/2018GL077207

Jiang, X., Waliser, D. E., Wheeler, M., Jones, C., Lee, M.-I., & Schubert, S. (2008). Assessing the skill of an all-season statistical forecast model for the Madden-Julian Oscillation. *Monthly Weather Review*, *136*, 1940–1956.

Kang, I., &Kim, H. (2010). Assessment of MJO Predictability for Boreal Winter with Various Statistical and Dynamical Models. *Journal of Climate*, *23*, 2368–2378. https://doi.org/10.1175/2010JCLI3288.1

Kiladis, G. N., Dias, J., Straub, K. H., Wheeler, M. C., Tulich, S. N., Kikuchi, K.,et al. (2014). A comparison of OLR andcirculation-based indices for tracking the MJO. *Monthly Weather Review*, *142* 1697–1715. https://doi.org/10.1175/MWR-D-13-00301.1

Lawrence, D. M., & Webster, P. J. (2002). The Boreal Summer Intraseasonal Oscillation: Relationship between Northward and Eastward Movement of Convection. *Journal of the Atmospheric Sciences*, *59*, 1593–1606. https://doi.org/10.1175/1520-0469(2002)059<1593:TBSIOR>2.0.CO;2

Lee, J. C. K., & Klingaman, N. P. (2018). The effect of the Quasi-Biennial Oscillation on the Madden-Julian Oscillation in the Met Office Unified Model Global Ocean Mixed Layer configuration. *Atmospheric Science Letters*, *19*(5). https://doi.org/10.1002/asl.816

Levene, H. (1960). Robust tests for equality of variances. In I. Olkin, H. Hotelling, et al. (Eds.), *Contributions to Probability and Statistics: Essays in Honor of Harold Hotelling*, (pp. 278–292). Palo Alto, CA: Stanford University Press.

Li, T., Wang, L., Peng, M., Wang, B., Zhang, C., Lau, W., & Kuo, H. (2018). A Paper on the Tropical Intraseasonal Oscillation Published in 1963 in a Chinese Journal. *Bulletin of the American Meteorological Society*, *99*(9), 1765–1779. https://doi.org/10.1175/BAMS-D-17-0216.1

Lim, Y., Son, S. W., Marshall, A. G., Hendon, H. H., & Seo, K. H. (2019). Influence of the QBO on MJO prediction skill in the subseasonal-to-seasonal prediction models. *Climate Dynamics*, *53*(3-4), 1681–1695. https://doi.org/10.1007/s00382-019-04719-y

Liu, F., Li, T., Wang, H., Deng, L., & Zhang, Y. (2016). Modulation of Boreal Summer Intraseasonal Oscillations over the Western North Pacific by ENSO. *Journal of Climate*, *29*(20), 7189–7201. https://doi.org/10.1175/JCLI-D-15-0831.1

Madden, R. A., & Julian, P. R. (1971). Detection of a 40-50 Day Oscillation in the Zonal Wind in the Tropical Pacific. *Journal of the Atmospheric Sciences*, *28*, 702–708. https://doi.org/10.1175/1520-0469(1971)028<0702:DOADOI>2.0.CO;2

Madden, R. A., & Julian, P. R. (1972). Description of Global-Scale Circulation Cells in the Tropics with a 40-50 Day Period. *Journal of the Atmospheric Sciences*, *29*, 1109–1123. https://doi.org/10.1175/1520-0469(1972)029<1109:DOGSCC>2.0.CO;2

Marshall, A. G., Hendon, H. H., Son, S.-W., & Lim, Y. (2017). Impact of the quasi-biennial oscillation on predictability of the Madden–Julian oscillation. *Climate Dynamics*, *49*(4), 1365–1377. https://doi.org/10.1007/s00382-016-3392-0

Martin, Z., Wang, S., Nie, J., & Sobel, A. (2019). The Impact of the QBO on MJO Convection in Cloud-Resolving Simulations. *Journal of the Atmospheric Sciences*, *76*(3), 669–688. https://doi.org/10.1175/JAS-D-18-0179.1

Nishimoto, E., & Yoden, S. (2017). Influence of the stratospheric quasi-biennial oscillation on the Madden–Julian oscillation during austral summer. *Journal of the Atmospheric Sciences*, *74*(4), 1105–1125. https://doi.org/10.1175/JAS-D-16-0205.1

Sobel, A. H., Maloney, E. D., Bellon, G.,&Frierson, D. M. (2010). Surface Fluxes and Tropical Intraseasonal Variability: a Reassessment. *Journal of Advances in Modeling Earth Systems*, *2*, 2. https://doi.org/10.3894/JAMES.2010.2.2

Son, S.-W., Lim, Y., Yoo, C., Hendon, H. H., & Kim, J. (2017). Stratospheric control of Madden–Julian oscillation. *Journal of Climate*, *30*(6), 1909–1922. https://doi.org/10.1175/JCLI-D-16-0620.1

Vitart, F. (2017). Madden—Julian Oscillation prediction and teleconnections in the S2S database. *Q.J.R. Meteorol Soc*, *143*(706), 2210–2220. https://doi.org/10.1002/qj.3079

Vitart, F., Ardilouze, C., Bonet, A., Brookshaw, A., Chen, M., Codorean, C., et al. (2017). The subseasonal to seasonal (S2S) prediction project database. *Bulletin of the American Meteorological Society*, *98*(1), 163–173. https://doi.org/10.1175/BAMS-D-16-0017.1

Wang, S., Ma, D., Sobel, A. H., & Tippett, M. K. (2018). Propagation characteristics of BSISO indices. *Geophysical Research Letters*, *45*(18), 9934–9943. https://doi.org/10.1029/2018GL078321

Wang, S., Sobel, A. H., Tippett, M. K., & Vitart, F. (2018). Prediction and predictability of tropical intraseasonal convection. *Climate Dynamics*, *52*(9-10), 6015–6031. https://doi.org/10.1007/s00382-018-4492-9

Wheeler, M. C., & Hendon, H. H. (2004). An All-Season Real-Time Multivariate MJO Index: Development of an Index for Monitoring and Prediction. *Monthly Weather Review*, *132*(8), 1917–1932. https://doi.org/10.1175/1520-0493(2004)132<1917:AARMMI>2.0.CO;2

Xie, Y.-B., Chen, S.-J., Zhang, I.-L., & Hung, Y.-L. (1963). A preliminarily statistic and synoptic study about the basic currents over southeastern Asia and the initiation of typhoon. *Acta Meteorologica Sinica*, *33*(2), 206–217. (in Chinese)

Yoo, C., & Son, S.-W. (2016). Modulation of the boreal wintertime Madden–Julian oscillation by the stratospheric quasi-biennial oscillation. *Geophysical Research Letters*, *43*, 1392–1398. https://doi.org/10.1002/2016GL067762

Zhang, C., & Zhang, B. (2018). QBO-MJO connection. *Journal of Geophysical Research: Atmospheres*, *123*(6), 2957–2967. https://doi.org/10.1002/2017JD028171